Late Quaternary activity along the Scorciabuoi Fault (Southern Italy) as inferred from electrical resistivity tomographies

Riccardo Caputo ([1]), **Luigi Salviulo** ([2])([3]), **Sabatino Piscitelli** ([4]) **and Antonio Loperte** ([4])

([1]) *Dipartimento di Scienze della Terra, Università degli Studi di Ferrara, Italy*

([2]) *Dipartimento di Strutture, Geotecnica, Geologia Applicata all'Ingegneria (DiSGG), Università degli Studi della Basilicata, Potenza, Italy*

([3]) *Dipartimento di Scienze Geologiche, Università degli Studi di Catania, Catania, Italy*

([4]) *Istituto di Metodologie per l'Analisi Ambientale (IMAA)-CNR, Tito Scalo (PZ), Italy*

Abstract

The Scorciabuoi Fault is one of the major tectonic structures affecting the Southern Apennines, Italy. Across its central sector, we performed several electrical resistivity tomographies with different electrode spacing (5 and 10 m) and using a multielectrode system with 32 electrodes. All tomographies were acquired with two different arrays, the dipole-dipole and the Wenner-Schlumberger. We also tested the different sensitivity of the two arrays with respect to the specific geological conditions and research goals. Detailed geological mapping and two boreholes were used to calibrate the electrical stratigraphy. In all but one tomography (purposely performed off the fault trace), we could recognise an abrupt subvertical lateral variation of the main sedimentary bodies showing the displacement and sharp thickening of the two youngest alluvial bodies in the hanging-wall block. These features are interpreted as evidence of synsedimentary activity of the Scorciabuoi Fault during Late Pleistocene and possibly as recently as Holocene and allow accurate location of the fault trace within the Sauro alluvial plain.

key words *active tectonics – Apennines – geoelectrical survey – Holocene – Val d'Agri*

1. Introduction

The present research is part of a multidisciplinary approach to the study of the Scorciabuoi Fault (Basilicata, Southern Italy) that affects the outer portion of the Lucanian Apennines, close to the boundary between the Apennine Chain and the Bradanic Foredeep (fig. 1a,b). This work is devoted to improving our knowledge concerning the seismic hazard of the Val d'Agri region. Although the whole area is characterized by a high seismic hazard (Gruppo di Lavoro, 2004), the principal seismotectonic parameters (position, length surface, geometry, etc.) of the potential seismogenic structures are not well defined (*e.g.,* Valensise and Pantosti, 2001a,b; Valensise *et al.*, 2003). Considering this scenario, the seismotectonic characterisation of the Scorciabuoi Fault could play an important role in the seismic hazard assessment of the broader region.

The principal aims of the multidisciplinary study are i) a description and the quantification of the Late Quaternary activity along the Scor-

Mailing address: Prof. Riccardo Caputo, Dipartimento di Scienze della Terra, Università degli Studi di Ferrara, Via Saragat 1, 44100 Ferrara, Italy; e-mail: rcaputo@unife.it

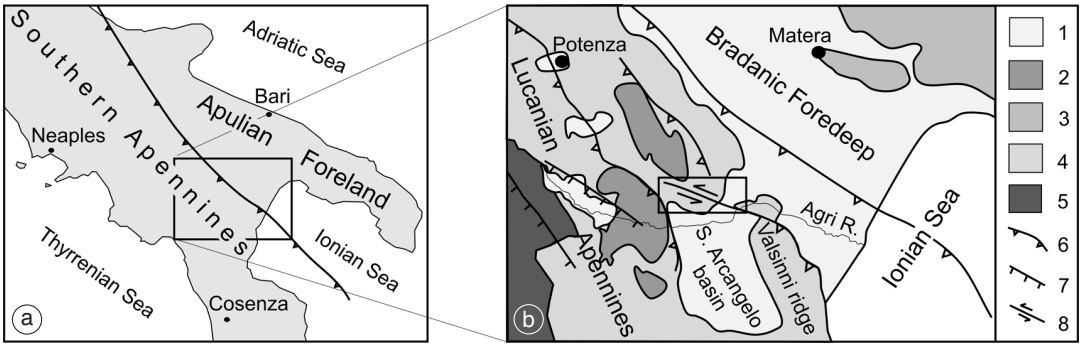

Fig. 1a,b. a) Location map of the investigated area in the frame of the Southern Apennines, Italy. The box in (b) indicates the area enlarged in fig. 2. Legend: 1 – clastic deposits of the Bradanic Foredeep (Pliocene-Quaternary); 2 – flysch deposits (Miocene); 3 – Lagonegro units (Lower Triassic-Middle Miocene); 4 – carbonate Apulian platform (Mesozoic-Cenozoic); 5 – carbonate Campania-Lucania platform (Mesozoic-Cenozoic); 6 – thrust faults; 7 – normal faults; 8 – strike-slip faults.

ciabuoi Fault and ii) an attempt to establish whether the fault could represent an important seismogenic structure in this sector of the Apennines and, specifically its possible relations with the 16 December 1857 (*M* 7.0) Great Neapolitan earthquake (Mallet, 1862; Boschi *et al.*, 2000). Accordingly, we carried out 1) a geological and structural investigation of the broader area, 2) a detailed morphological analysis of the fluvial terraces crossed by the fault, 3) numerical simulations of the vertical movements associated with the Scorciabuoi Fault and 4) a geoelectrical resistivity survey focused on the central sector of the fault. This paper presents the results of the latter geophysical investigation which essentially deal with aim (ii), while the Late Quaternary activity is discussed in more detail by Caputo and Salviulo (2005).

2. Geological framework

The Sant'Arcangelo marine basin represents the most recent piggy-back basin of the Southern Apennines. It is located close to the outer portion of the Lucanian Apennine Chain, west of the Bradanic Foredeep. The Sant'Arcangelo Basin developed on top of the allochthonous units as a thrust-top basin during the latest stages of the Apennines compression and evolved, in the Early-Middle Pleistocene, to a piggy-back basin (Pieri *et al.*, 1994; Monaco *et al.*, 1998). This evolution was controlled by the rising of the Valsinni ridge that produced a satellite basin separated from the Bradanic Foredeep (Patacca and Scandone, 2001).

The basin shows a synform geometry and the sedimentary infilling consists of a thick siliciclastic sequence of Pliocene-Quaternary marine and continental deposits characterised by a general shallowing upwards trend. The youngest deposits are represented by the Middle Pleistocene Serra Corneta Unit (Vezzani, 1967; Pieri *et al.*, 1994) and consist of conglomerates and sands.

According to Pieri *et al.* (1994), the stratigraphic setting of the basin consists of four depositional sequences whose age is Late Pliocene-Middle Pleistocene. These sequences are separated from one another by unconformities, some of them being of clear syntectonic nature.

The Scorciabuoi Fault is *ca*. 30 km long, with a WNW-ESE trend and represents the northern border of the Middle Pliocene-Middle Pleistocene Sant'Arcangelo piggy-back basin (figs. 1a,b and 2). The fault crosses the central sector of the Sauro Valley, a major tributary of the Agri River. Notwithstanding its young age, the fault shows evidence of a double kinematics. Indeed, the structure formed in Early Pleistocene time (Catalano *et al.*, 1993; Pieri *et al.,*

1994; Casciello, 2002; Patacca and Scandone, 2001) as an oblique-lateral ramp linked to the Valsinni frontal-ramp anticline during the major eastward thrusting. However, from 0.7-0.5 Ma onwards, the internal sectors of the Apennines Chain have been affected by a general (E)NE-(W)SW trending extension and the Scorciabuoi Fault was inverted and reactivated as a normal fault (Pieri *et al.*, 1997).

Based on literature data and original field mapping, the structural characteristics of the Scorciabuoi Fault have been analysed in detail and are more extensively described in Caputo and Salviulo (2005). It is noteworthy that from a structural point of view the fault can be clearly recognised and mapped both northwest and southeast of the Sauro Valley (fig. 2). In between, the Sauro Valley is mainly covered by Middle *pp*-Late Quaternary (*i.e.* post-Serra Corneta Unit) loose or poorly consolidated alluvial deposits and no clear surface evidence of the fault trace could be observed.

In this sector of the valley, four orders of fluvial terraces and the corresponding alluvial bodies were recognised (Caputo and Salviulo, 2005). In particular, within the investigation site (Acinello plain; fig. 3a,b), the two most recent terraces (T1 and T2) have been mapped, while the geological substratum of the alluvial cover is locally represented by the marly clays of the Caliandro Cycle (Upper Pliocene).

In order to document the recent tectonic activity of the Scorciabuoi Fault, we carried out a geophysical survey based on the electrical resistivity measurement of the surface sedimentary units across the possible fault trace. Indeed, if the Scorciabuoi Fault is active and was re-activated several times during the Late Pleistocene and possibly the Holocene, a cumulative and differential deformation of the terraced alluvial bodies has certainly occurred. Based on this geophysical approach, the final aim of this research is to document the occurrence of recent linear morphogenic earthquakes that is ca-

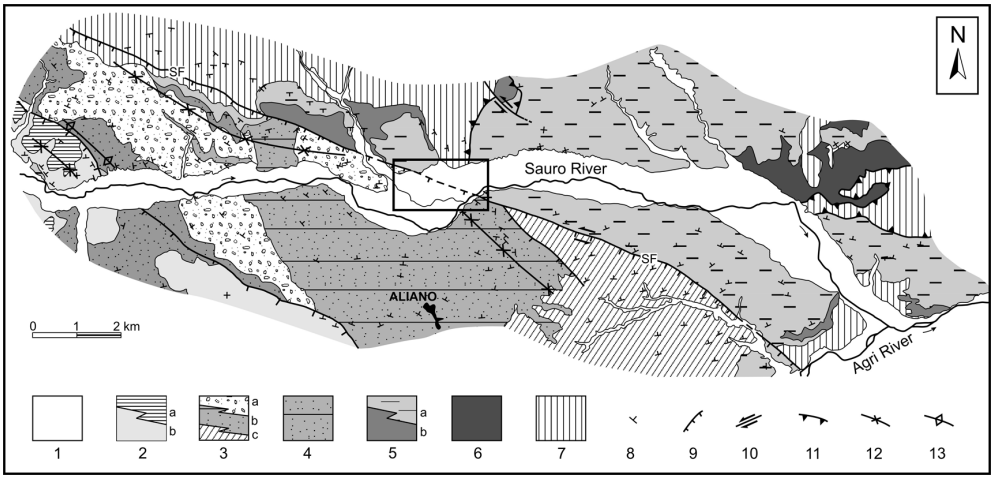

Fig. 2. Simplified geological map of the Sauro Valley, Southern Apennines (Italy). See location in fig. 1b. Legend: 1 – alluvial deposits (uppermost Pleistocene-Holocene); 2 – San Lorenzo Cycle (Middle Pleistocene; a: silty claystones; b: conglomerates); 3 – Sauro Cycle (Early-Middle Pleistocene; a: conglomerates; b: sandstones; c: silty claystones); 4 – Agri Cycle (Late Pliocene-Early Pleistocene): sandstones; 5 – Caliandro Cycle (Late Pliocene; a: marly claystones; b: conglomerates and sandstones); 6 – Lower Pliocene Clays; 7 – pre-Pliocene Units; 8 – bedding; 9 – normal fault (barbs on the downthrown side); 10 – strike-slip fault (Pliocene-Middle Pleistocene kinematics); 11 – thrusts (triangles on the hanging-wall); 12 – syncline axis; 13 – anticline axis. The box indicates the area enlarged in fig. 3a.

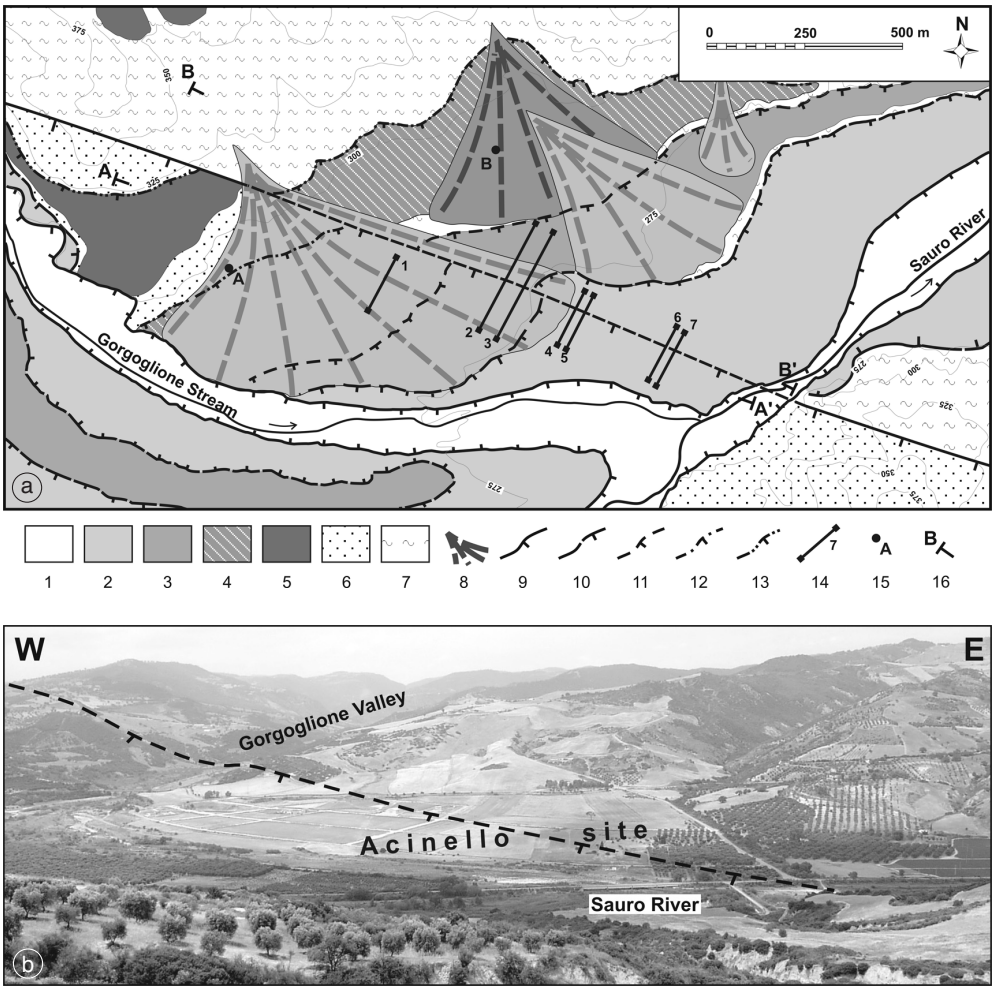

Fig. 3a,b. a) Simplified morphotectonic map of the Acinello site where the geophysical survey has been carried out. The location of the seven ERTs is indicated. 1 – present-day alluvial terrace (T0); 2 – terrace T1; 3 – terrace T2; 4 – terrace T3; 5 – terrace T4; 6 – Sauro Cycle deposits; 7 – Caliandro Cycle deposits; 8 – alluvial cones (the colour indicates the relative age with respect to the terraces); 9 – inner edge of T0; 10 – inner edge of T1; 11 – inner edge of T2; 12 – inner edge of T3; 13 – inner edge of T4; 14 – trace of the electrical resistivity tomographies; 15 – location of the bore-holes; 16 – location of the geological profiles shown in fig. 8. b) Panoramic view (from south to north) of the investigated site.

pable of generating, or modifying, the surface morphology instantaneously and permanently as a consequence of the upward propagation of a co-seismic displacement and its resulting ground rupture (Caputo, 2005).

3. Electrical Resistivity Tomographies

Electrical Resistivity Tomography (ERT) is an active geoelectrical prospecting technique used to acquire 2D and 3D high-resolution im-

ages of the electrical resistivity pattern of the subsurface (Griffiths and Barker, 1993; Loke and Barker, 1996). This technique has been recently and successfully used to solve a wide range of geological problems, like the recognition of structural settings within volcanic areas (Di Maio *et al.*, 1998), monitoring of groundwater pollution (Ogilvy *et al.*, 1999), investigation of geological structures of the upper crust (Giano *et al.*, 2000; Storz *et al.*, 2000; Suzuki *et al.*, 2000; Caputo *et al.*, 2003) and the identification of sliding surfaces in landslides (Gallipoli *et al.*, 2000; Lapenna *et al.*, 2003, 2005).

Electrical resistivity measurements can be acquired using different electrode configurations (dipole-dipole, Wenner, pole-pole, Wenner-Schlumberger, etc.) characterized by different geometrical factors (k) defining the distribution of the electrodes (fig. 4). In 2D tomographies the energizing and receiving systems are moving along a fixed profile and thus it is possible to describe the lateral and vertical variations of the apparent resistivity. The profile acquisition can be entirely performed by a computer programme that automatically determines a 2D resistivity model of the subsurface (pseudo-section) based on the data obtained from electrical imaging surveys (Griffiths and Barker, 1993). Note that this model is characterized by apparent resistivity values, because the program defines only a theoretical distribution of the resistivity in the ground.

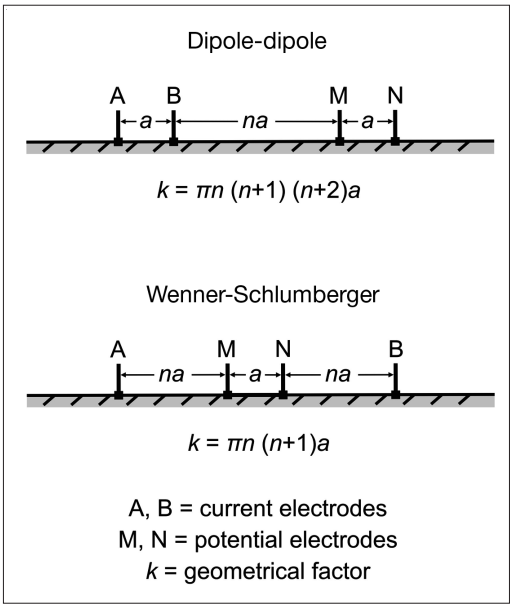

Fig. 4. The two electrodes arrays used in the geoelectrical investigation.

As a second step, pseudo-sections need to be inverted in real resistivity values. The 2D resistivity model used by the inversion programme consists of a number of rectangular blocks whose arrangement is loosely tied to the distribution of the data points in the pseudo-section. The distribution and size of the blocks mimic the distribution of the data points measured in the field. The deepest line of blocks is assumed equal to the equivalent depth of investigation of the data points with the largest electrode spacing (Edwards, 1977). The inversion routine generally used is a non-linear least-square *quasi*-Newton optimisation technique (deGroot-Helding and Constable, 1990; Loke and Barker, 1996). The optimisation procedure fixes the 2D resistivity model using an iterative process to reduce the difference between calculated and measured apparent resistivity values. The inversion programme also provides the corresponding RMS error, giving a measure of the reliability of the final result.

During the geophysical study of the Scorciabuoi Fault, seven profiles were acquired so that different tomographies could be prepared. Each resistivity profile was carried out with two different electrode settings: the dipole-dipole array and the Wenner-Schlumberger array (fig. 4). Note that this research also represents an attempt to test these techniques when applied to geological conditions like the investigated one, characterised by horizontal bodies (*viz.* alluvial deposits) and a subvertical discontinuity (*viz.* fault). For the dipole-dipole array (fig. 4), the spacing between the current electrodes pair (A-B) and the potential electrodes pair (M-N) is the same and equal to a. The factor n is the ratio between the distance of the B-M electrodes and a. For surveys with this array, the length of a is initially kept fixed at the smallest unit electrode spacing, while n is progressively increased from 1 to about 6 in order to increase the depth of investigation.

The Wenner-Schlumberger array (fig. 4) is a new hybrid method, mixing both Wenner and Schlumberger arrays. The *n* factor for this array corresponds to the ratio between the distance of the B-N (or M-A) electrodes and the spacing between the M-N potential electrodes pair.

The basic difference between the dipole-dipole and the Wenner-Schlumberger arrays is in the principal direction of sensitivity. The former detects small horizontal changes in resistivity, but it is relatively insensitive to vertical changes in the resistivity. In contrast, the second array is moderately sensitive to both horizontal and vertical structures. Accordingly, the dipole-dipole array is powerful for mapping vertical structures such as faults, dykes and cavities, but a relatively weak method for mapping horizontal structures like sills or layering.

4. ERTs at Acinello site

At the Acinello site, the location of the electrical tomographies was preliminarily determined on the basis of the likely trace of the Scorciabuoi Fault across the Late Quaternary alluvial deposits of the Sauro Valley (figs. 2 and 3a,b). Seven parallel tomographies have been oriented roughly

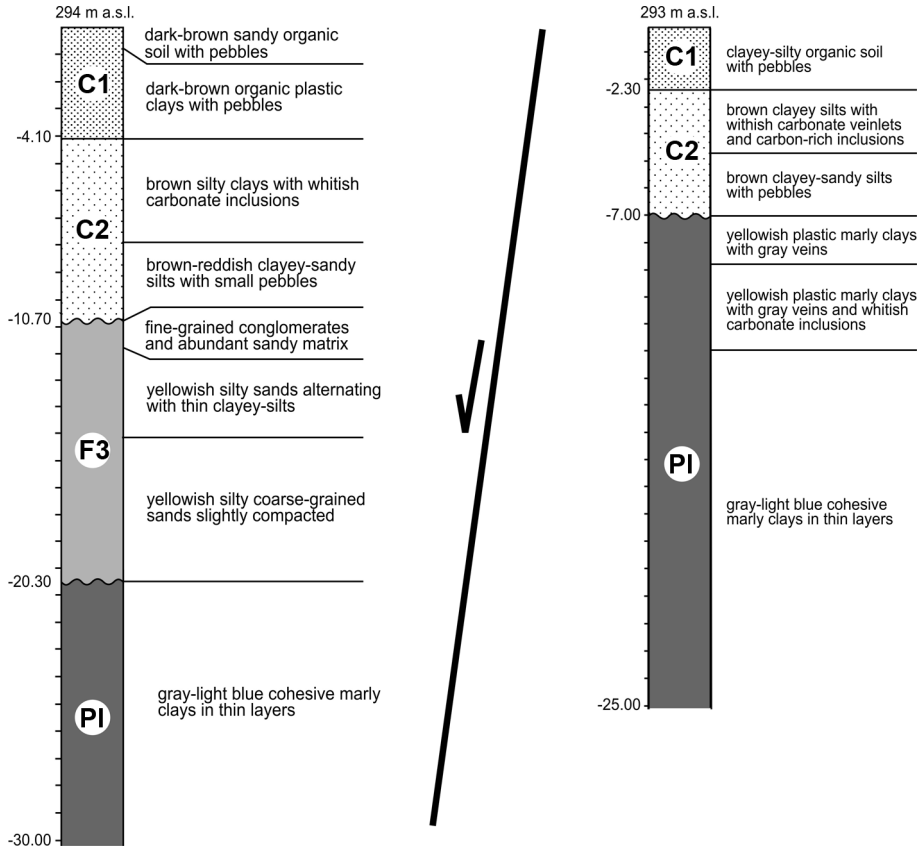

Fig. 5. The two stratigraphic boreholes used to calibrate the electrical resistivity tomographies. For location see fig. 3a,b. F_n – alluvial body associated with terrace T_n; C_n – alluvial cone associated with the fluvial body F_n; Pl – Pliocene marls-clays of the Caliandro Cycle.

perpendicular to the possible fault trace and carried out using a multi-electrode system with 32 electrodes. Five profiles were characterized by 5 m electrode spacing, the remaining two by a 10 m inter-electrode distance. The two types of profiles are 155 and 310 m long, respectively. Obviously, resolution is higher in the former (Loke, 2001; Caputo *et al.*, 2003), while the depth of investigation is greater in the latter. To validate the whole procedure and the results obtained, one of the tomographies (ERT1) was deliberately located outside the likely fault trace (fig. 3a). The remaining six profiles were carried out as three pairs of tomographies at 50 m (ERT2-ERT3) and 25 m distance (ERT4-ERT5 and ERT6-ERT7), for the 10 and 5 m inter-electrode spacing, respectively (fig. 3a). Although the inversion method provides RMS values, the selected technique to repeat the profiles at relatively short distance is probably the best way to test the reliability of the obtained results (Caputo *et al.*, 2003).

For the geoelectrical survey, we used the Georesistivimeter Syscal R2 of Iris Instruments, while we carried out the subsequent data inversion with the RES2DINV software (Loke and Barker, 1996).

Measured resistivities in all seven tomographies are within a range of low absolute values (*ca*. 5-150 Ωm), therefore in good agreement with the lithological characteristics of the alluvial deposits of the plain. In particular, the lowest resistivity values correspond to clays or argillaceous-silty deposits, while the highest measured resistivity values are associated with sand-conglomerate alluvial bodies. In this regard, by using the stratigraphic sequence shown in two boreholes drilled on the two sides of the fault trace near our tomographies (fig. 3a), it is possible to calibrate the results of the geophysical survey and to directly correlate resistivity values with the lithostratigraphic characteristics. The detailed lithostratigraphic column of the two boreholes, with a brief description of the drilled deposits, is represented in fig. 5.

5. Discussion

The tomographies acquired with the dipole-dipole array are potentially more meaningful for the purpose of the present research devoted to identifying the recent morphogenic activity of the Scorciabuoi Fault. The resistivity patterns obtained with the Wenner-Schlumberger array are generally more flattened and therefore the resulting tomographies do not facilitate the subsurface interpretation and the characterization of the subvertical discontinuity (*viz.* fault). Accordingly, in the following discussion we focus on the dipole-dipole tomographies and the consequent geological interpretation is mainly based on this geophysical method. The seven tomographies carried out across the Scorciabuoi Fault are shown in fig. 6, while the corresponding geological interpretations based on i) the distribution of the resistivity bodies, ii) the lithostratigraphic columns obtained from the boreholes (fig. 5) and iii) the surface geology (figs. 2 and 3a,b) are represented in fig. 7.

Six out of the seven sections (ERT2 to ERT7; figs. 6 and 7) clearly show the occurrence of a lateral discontinuity exactly at the intersection with the likely trace of the Scorciabuoi Fault. In these sections, at a depth of 15-20 m from the surface, a relatively high-conductive body (< *ca*. 15 Ωm) occurs in the footwall block and it is referred to the uplifted pelitic unit of the Caliandro Cycle (Upper Pliocene; Pl in figs. 6 and 7). This conductive body does not continue southwestwards (*viz.* hanging-wall block) and in the deeper tomographies (ERT2 and ERT3) its abrupt termination is quite evident. Both surface data (fig. 3a,b) and the stratigraphic information available from the boreholes (fig. 5) unambiguously confirm the occurrence at depth of the grey-light blue cohesive marly clays belonging to the Caliandro Cycle. The subsurface data also clearly emphasise the difference in depth of the top erosional surface of this formation (fig. 5).

In the same six tomographies and overlying the Pl unit, there is a second horizontal electrical body characterised by resistivity values between 15 and 50 Ωm. This electrical unit is interpreted as the alluvial body associated with the fluvial terrace 2 (respectively F2 and T2 in figs. 3a,b, 6 and 7). Also in this case, it is possible to observe a sharp lateral thickness variation, from 10-15 m in the northeastern sector to 30+ m in the southwestern sector. The top of

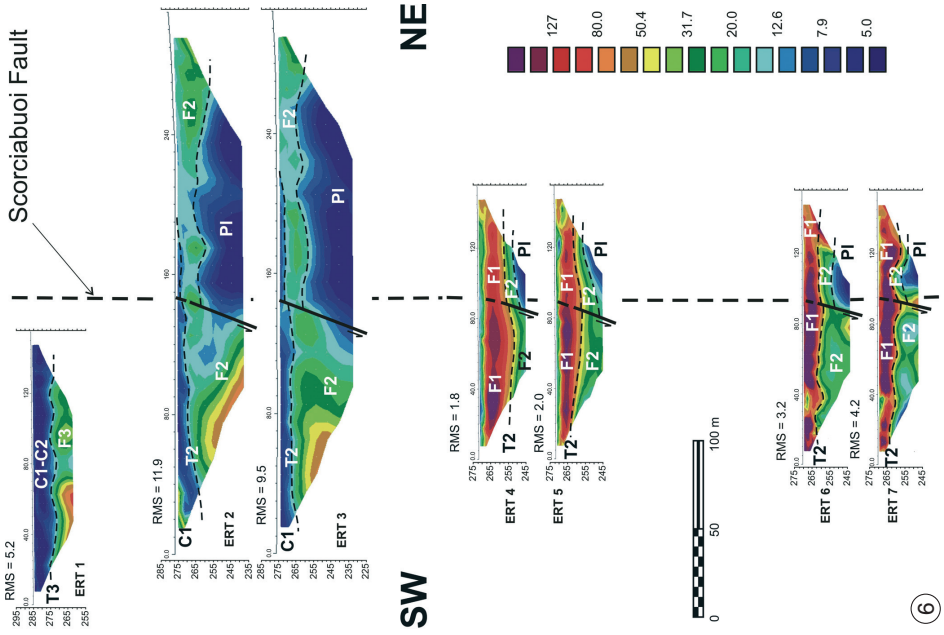

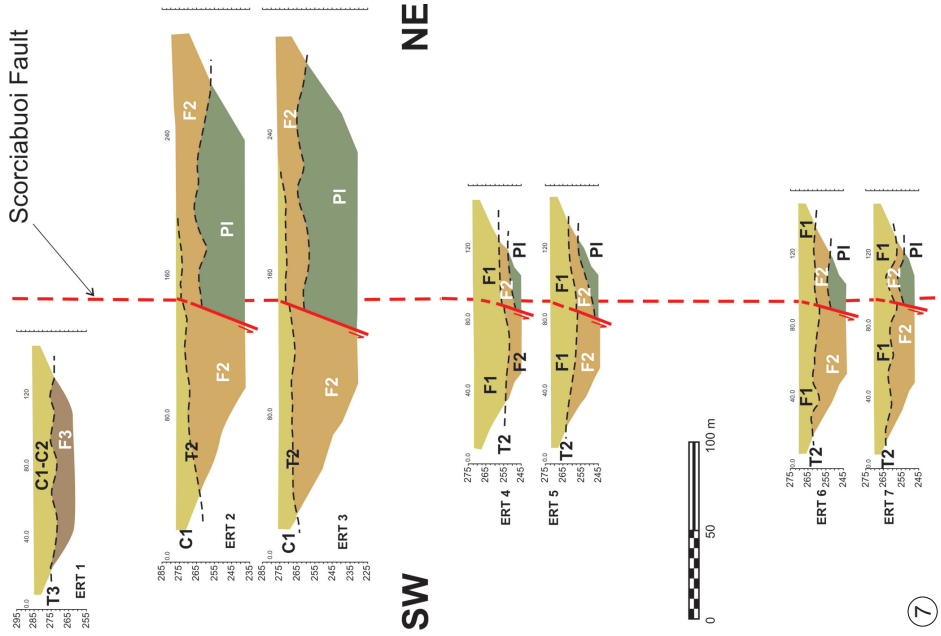

Fig. 6. The seven electrical resistivity tomographies carried out across the Scorciabuoi Fault at the Acinello site. Resistivity values are in Ωm. Symbols as in fig. 3a,b and 5.

Fig. 7. The seven geological profiles as inferred from the electrical resistivity tomographies (fig. 6), the stratigraphic boreholes (fig. 5) and the surface geology (figs. 2 and 3a,b). Symbols as in fig. 3a,b and 5.

this unit (surface T2) is also slightly downthrown in the southwestern block (*i.e.* hanging-wall).

In the four southeastern tomographies (ERT4 to ERT7; fig. 6), a third and younger electrical unit characterised by the locally highest resistivity values (>50-60 Ωm) can be also recognised. Its thickness varies between 10-15 m, to the NE, and 15-20 m, to the SW. Similar to the underlying unit, though less important, the thickness variation seems to occur in correspondence with the fault intersection. Based on surface data, this electrical unit represents the alluvial body associated with the lowest fluvial terrace (respectively F1 and T1 in figs. 3a,b, 6 and 7).

Close to the inner-edge of the terraced surface T1 (ERT4 and ERT5; fig. 3a,b), unit F1 is partly overlain by a relatively more conductive thin layer (2-3 m) of colluvial-alluvial deposits probably washed out from the nearby morphological scarp and/or from the alluvial cones fed by the northern slope (C1 in fig. 3a,b). Indeed, higher conductivity values characterising the alluvial cones are also well documented in the three westernmost tomographies (ERT1 to ERT3; figs. 3a,b and 6), where southwest of the fault trace it is possible to observe a 10-15 m thick unit (<*ca*. 15 Ωm). As expected, this unit progressively thickens northwest (compare ERT2-3 with ERT1), that is towards the source area of the alluvial cone. This electrical unit

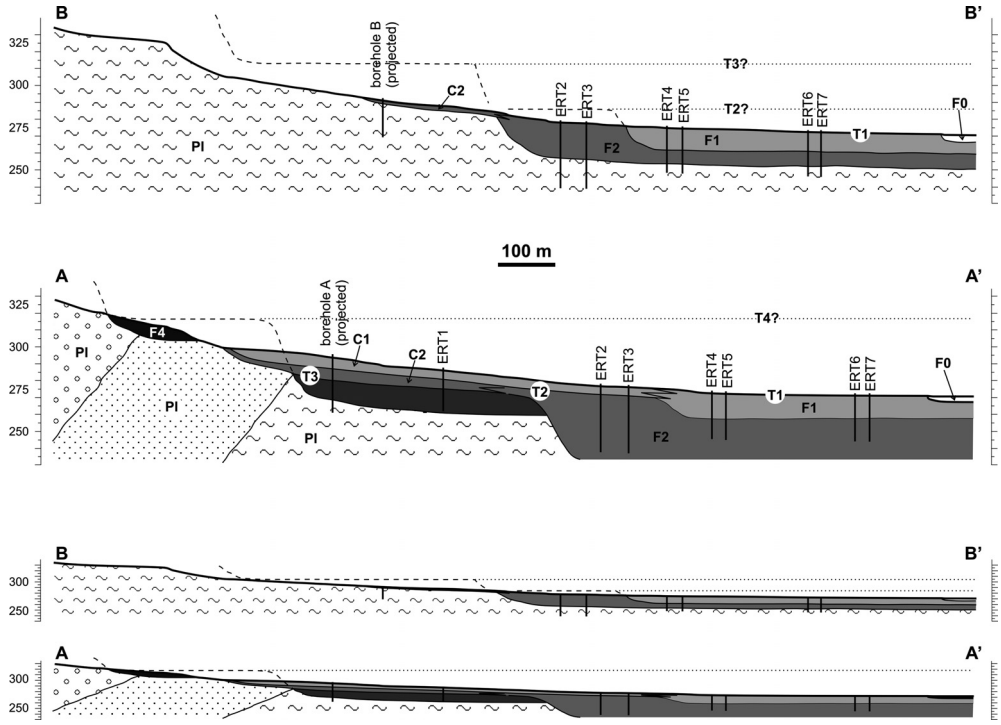

Fig. 8. Geological profiles parallel to the Scorciabuoi Fault and running immediately SW (A-A′) and NE (B-B′) of the fault trace across the Sauro Valley. Profiles location is in fig. 3a,b, while symbols are as in fig. 5. The two upper profiles have a vertical exaggeration of 3:1, while the below ones are the same shown with no vertical exaggeration.

was also drilled by borehole A, whose stratigraphic column clearly documents the occurrence of clays and silty clays with pebbles up to a depth of *ca*. 10 m (fig. 5). This material likely represents the two superposed alluvial cones C2 and C1, though the applied geophysical method does not allow to separate them because of the similar resistivity behaviour.

As mentioned above, to validate the results, we carried out one profile entirely located off the fault trace (ERT1; fig. 3a,b). As expected, this tomography does not show any significant lateral discontinuity or any lateral variation in resistivity. In contrast, a regular horizontal distribution of the resistivity layering can be observed with the separation of two electrical units. In particular, the first layer corresponds to the sediments belonging to the superposed alluvial cones C2 and C1, characterised by low resistivity values (< *ca*. 15 Ωm), while the second layer shows a relatively higher resistivity and this unit likely corresponds to the alluvial body associated with the fluvial terrace 3 (respectively F3 and T3 in figs. 3a,b, 6 and 7). This interpretation is confirmed by borehole A (fig. 5), where at a depth of about 10 m, the boundary between the conductive and poorly sorted alluvial cone deposits (C1 and C2) and the mainly sandy-conglomerate alluvial sediments (F3) overlying the marly clays of the Caliandro Cycle can be observed (Upper Pliocene; Pl in fig. 5).

As a final comment, the RMS values obtained from the numerical inversion are satisfactorily low in all seven tomographies, with values below 5.2, in the shorter ones, and around 10, in the longer ones characterised by a greater inter-electrode distance (*viz.* uncertainty). The overall picture confirms the reliability of the obtained result.

The alternative hypothesis that the lateral variation observed in the ERTs, and particularly the disappearance of the Upper Pliocene deposits southwest of the fault trace, is due to an erosional scarp that was filled during Late Pleistocene is unlikely. This is due to the high erodibility of the marls-clays of the Caliandro Cycle, as easily observed in surrounding outcrops, which could not generate similar erosional scarps standing, with an high-angle slope and tens of meters high, for tens of ka before their complete burial under the overlapping fluvial sediments. Moreover, the top surface of the subsequent fluvial bodies that covered this hypothetical erosional feature should have a flat morphology as a consequence of the alluvial depositional mechanism. Such morphology is not observed in our tomographies, at least as concerns terrace T2 (figs. 6 and 7).

On the other hand, based on the subsurface (ERTs and boreholes; figs. 5 and 6) and surface (fig. 3a,b) data, two geological profiles running close, parallel and on the two sides of the fault trace (fig. 8) help shed light on the role played by the Scorciabuoi Fault during the Late Quaternary evolution of the Sauro valley. In the northeastern profile (*i.e.* footwall block), the different terraced surfaces show large altimetric differences, while in the southwestern profile (hanging-wall block), the three younger terraced surfaces (T1-T3) have closer altitudes. Accordingly, the different distribution of the recognised alluvial bodies and terraces suggests that the locally induced tectonic subsidence almost compensated the regional uplift, therefore confirming the importance of the fault as a Late Quaternary morphogenic structure.

6. Concluding remarks

The analysis of the results obtained from the geoelectrical survey and their geological interpretation clearly documents the Late Quaternary activity of the Scorciabuoi Fault for the first time. In particular, the six tomographies crossing the fault trace provide evidence of a linear morphogenic activity, which was synsedimentary with the formation of the Upper Pleistocene terraced alluvial deposits observed along the Sauro valley. Indeed, the younger is the affected sedimentary unit, the smaller is the amount of observed displacement (figs. 6 and 7). For example, the base of unit F2 underwent more than 25-30 m of down-dip slip, while this value drops to less than 10 m for the top of the same unit (ERT2-ERT3; figs. 6 and 7). Also, the youngest observed alluvial body F1 shows a few metres of displacement at the base, while the top surface seems to be almost unaffected,

at least within the available resolution of the geoelectrical investigation method (ERT4 to ERT7; figs. 6 and 7).

If the trace of the Scorciabuoi Fault across the Sauro Valley was only hypothetical before this study, another important outcome of the present research is the possibility to have exactly located it within the alluvial plain. This information will be crucial for palaeoseismological investigations, the only methodological approach that could definitely document the occurrence of Holocene morphogenic earthquakes and possibly verify whether the Scorciabuoi Fault was reactivated during the 1857 Val d'Agri earthquake.

Whatever the case, our results show the occurrence of recent (Late Pleistocene at least) reactivations of the Scorciabuoi Fault. If future earthquakes will reactivate the entire fault length (*ca*. 30 km), the associated magnitude could range between 6.7 and 6.9 (Pavlides and Caputo, 2004) and the seismic potential will be significant. Accordingly, the seismic hazard induced by the Scorciabuoi Fault is not negligible and further research should be devoted to a quantitative assessment.

Acknowledgements

Research carried out in the frame of the Italian Department Civil Protection-INGV project (resp. RC). Thanks to U. Fracassi and an anonymous reviewer for improving a first version of the paper.

REFERENCES

Boschi, E., E. Guidoboni, G. Ferrari, D. Mariotti, G. Valensise and P. Gasperini (Editors) (2000): Catalogue of strong Italian earthquakes from 461 B.C. to 1997, *Ann. Geofis.*, **43** (4), 609-868 (with CD-ROM).

Caputo, R. (2005): Ground effects of large morphogenic earthquakes, *J. Geodyn.*, **40** (2-3), 113-118.

Caputo, R. and L. Salviulo (2005): Late Quaternary activity of the Scorciabuoi Faul, Southern Italy, in *Proceedings of the 14th Meeting Ass. European Geological Societies*, Torino, September 19-23, 2005, (abstract), 53-55.

Caputo, R., S. Piscitelli, A. Oliveto, E. Rizzo and V. Lapenna (2003): The use of electrical resistivity tomographies in active tectonics: examples from the Tyrnavos Basin, Greece, *J. Geodyn.*, **36**, 19-35.

Casciello, E. (2002): Deformazioni da taglio in materiali argillosi: analisi dei sedimenti deformati dalla faglia di Scorciabuoi, *Studi Geologici Camerti*, **1**, 51-62.

Catalano, S., C. Monaco, L. Tortorici and C. Tansi (1993): Pleistocene strike-slip tectonics in the Lucanian Apennine (Southern Italy), *Tectonics*, **12** (3), 656-665.

deGroot-Hedlin, C. and S. Constable (1990): Occam's inversion to generate smooth, two-dimensional models from magnetotelluric data, *Geophysics*, **55**, 1613-1624.

Di Maio, R., P. Mauriello, D. Patella, Z. Petrillo, S. Piscitelli and A. Siniscalchi A. (1998): Electric and electromagnetic outline of the Mount Somma-Vesuvius structural setting, *J. Volcanol. Geotherm. Res.*, **82** (1-4), 219-238.

Edwards, L.S. (1977): A modified pseudosection for resistivity abd induced polarization, *Geophysics*, **42**, 1020-1036.

Gallipoli, M.R., V. Lapenna, P. Lorenzo, M. Mucciarelli, A. Perrone, S. Piscitelli and F. Sdao (2000): Comparison of geological and geophysical prospecting techniques in the study of a landslide in Southern Italy, *Eur. J. Environ. Eng. Geophys.*, **4**, 117-128.

Giano, S.I., V. Lapenna, S. Piscitelli and M. Schiattarella (2000): Electrical imaging and self-potential surveys to study the geological setting of the Quaternari slope deposits in the Agri high valley (Southern Italy), *Ann. Geofis.*, **43** (2), 409-419.

Griffiths, D.H. and R.D. Barker (1993): Two-dimensional resistivity imaging and modelling in areas of complex geology, *J. Appl. Geophys.*, **29**, 211-226.

Gruppo di Lavoro (2004): Redazione della mappa di pericolosità sismica prevista dall'Ordinanza PCM 3274 del 20 marzo 2003, *Final Report for the Italian Department of Civil Protection*, INGV, April 2004, Milan-Rome, pp. 65 (5 Appendixes).

Lapenna, V., P. Lorenzo, A. Perrone, S. Piscitelli, F. Sdao and E. Rizzo (2003): High-resolution geoelettrical tomographies in the study of Giarrossa landslide (Southern Italy), *Bull. Eng. Geol. Environ.*, **62**, 259-268.

Lapenna, V., P. Lorenzo, A. Perrone, S. Piscitelli, F. Sdao and E. Rizzo (2005): 2D electrical resistivity imaging of some landslides in Lucanian Apennine (Southern Italy), *Geophysics*, **70** (3), B11-B18, doi: 10.1190/1.1926571.

Loke, M.H. (2001): Tutorial: 2D and 3D electrical imaging surveys, in *Course Notes for USGS Workshop '2D and 3D Inversion and Modeling of Surface and Borehole Resistivity Data'*, 13-16 March 2001, Storrs, CT.

Loke, M.H. and B.D. Barker (1996): Rapid least-squares inversion of apparent resistivity pseudosections by a *quasi*-Newton method, *Geophys. Prospect.*, **44**, 131-152.

Mallet, R. (1862): *Great Neapolitan Earthquake of 1857. The First Principles of Observational Seismology as Developed in the Report to the Royal Society of London* (Chapman and Hall), 2 vols., pp. 431

Monaco, C., L. Tortorici and W. Paltrinieri (1998): Structural evolution of the Lucanian Apennines, Southern Italy, *J. Struct. Geol.*, **20** (5), 617-638.

Ogilvy, R., P. Meldrum and J. Chambers (1999): Imaging of industrial waste deposits and buried quarry geometry by 3D resistivity tomography, *Eur. J. Environ. Eng. Geophys*., **3**, 103-113.

PATACCA, E. and P. SCANDONE (2001): Late thrust propagation and sedimentary response in the thrust-belt-foredeep system of the Southern Apennines (Pliocene-Pleistocene), in *Anatomy of an Orogene: the Apennines and Adjacent Mediterranean Basin*, edited by G.B. VAI and P. MARTINI (Kluwer Academic Publishers), 401-440.

PAVLIDES, S. and R. CAPUTO (2004): Magnitude *versus* faults' surface parameters: quantitative relationships from the Aegean region, *Tectonophys*, **380** (3-4), 159-188, doi: 10.1016/j.tecto.2003.09.019.

PIERI, P., L. SABATO, F. LOIACONO and M. MARINO (1994): Il bacino di piggyback di Sant'Arcangelo: evoluzione tettonico-sedimentaria, *Mem. Soc. Geol. It.*, **113**, 465-481.

PIERI, P., G. VITALE, P. BENEDUCE, C. DOGLIONI, S. GALLICCHIO, S.I. GIANO, R. LOIZZO, M. MORETTI, G. PROSSER, L. SABATO, M. SCHIATTARELLA, M. TRAMUTOLI and M. TROPEANO (1997): Tettonica Quaternaria nell'area Bradanico-Ionica, *Il Quaternario*, **10** (2), 535-542.

STORZ, H., W. STORZ and F. JACOBS (2000): Electrical resistivity tomography to investigate geological structures of the Earth's upper crust, *Geophys. Prosp.*, **48**, 455-471.

SUZUKI, K., S. TODA, K. KUSUNOKI, Y. FUJIMITSU, T. MOGI and A. JOMORI (2000): Case studies of electrical and electromagnetic methods applied to mapping active faults beneath the thick quaternary, *Eng. Geol.*, **56**, 29-45.

VALENSISE, G. and D. PANTOSTI (Editors) (2001a): Database of potential sources for earthquakes larger than *M* 5.5 in Italy, *Ann. Geofis.*, **44** (4), 797-807.

VALENSISE, G. and D. PANTOSTI (2001b): The investigation of potential earthquake sources in peninsular Italy: a review, *J. Seismol.*, **5**, 287-306.

VALENSISE, G., A. AMATO, P. MONTONE and D. PANTOSTI (2003): Earthquakes in Italy: past, present and future, *Episodes*, **26** (3), 245-249.

VEZZANI, L. (1967): Il bacino Plio-Pleistocenico di S. Arcangelo (Lucania), *Atti Acc. Gioenia Sc. Nat. Catania*, **18**, 207-227.

(received September 18, 2006;
accepted February 15, 2007)